

ELECTRONIC PROPERTIES OF RANDOM POLYMERS: MODELLING OPTICAL SPECTRA OF MELANINS

KINGA BOCHENEK AND EWA GUDOWSKA-NOWAK

M. Smoluchowski Institute of Physics, Jagellonian University
Reymonta 4, 30-059 Kraków, Poland

e-mail: kinga@indigo.if.uj.edu.pl
gudowska@th.if.uj.edu.pl

(Received November 25, 2002)

Melanins are a group of complex pigments of biological origin, widely spread in all species from fungi to man. Among diverse types of melanins, the human melanins, *eumelanins*, are brown or black nitrogen-containing pigments, mostly known for their photoprotective properties in human skin. We have undertaken theoretical studies aimed to understand absorption spectra of *eumelanins* and their chemical precursors. The structure of the biopigment is poorly defined, although it is believed to be composed of cross-linked heteropolymers based on indolequinones. As a basic model of the *eumelanin* structure, we have chosen pentamers containing hydroquinones (HQ) and/or 5,6-indolequinones (IQ) and/or semiquinones (SQ) often listed as structural melanin monomers. The *eumelanin* oligomers have been constructed as random compositions of basic monomers and optimized for the energy of bonding. Absorption spectra of model assemblies have been calculated within the semiempirical intermediate neglect of differential overlap (INDO) approximation. Model spectrum of eumelanin has been further obtained by sum of independent spectra of singular polymers. By comparison with experimental data it is shown that the INDO/CI method manages to reproduce well characteristic properties of experimental spectrum of synthetic *eumelanins*.

PACS numbers: 87.15.-v, 31.10.+z, 31.15.Gy, 36.20-r

1. Introduction

Melanins are ubiquitous natural pigments formed by oxidation and polymerization of catechols [1, 2]. Black or dark brown nitrogen-containing melanins are classified as *eumelanins* distinctly from *pheomelanins* — whose

lighter coloring originates from intervention of cysteine in the process of melanogenesis, and *allomelanins* — which originate from nitrogen-free precursors and are typical of plants and microorganisms. The *melanogens*, uncolored precursors of melanins of the animal kingdom, are diphenols derived from phenylalanine and from tyrosine. The melanin pigments are amorphous substances of remarkable ability to absorb almost indiscriminately near-infrared, visible and ultraviolet radiation [2,3]. Exploiting these properties of melanins has proven to be a complex task, since despite significant experimental effort on a variety of natural and synthetic melanins, the molecular structure of the pigment and its organization remains still unknown. Poorly understood are also functional properties of natural melanin pigments which call for attention because of their both photoprotective and photosensitizing properties.

In this paper we will focus on hypothesis which concludes on spectroscopic properties of melanins assuming their polymeric amorphous structure. Our studies concern *eumelanins* which are known as complex broadband absorbers, frequently subject to excitation in its native environments. Eumelanin is mainly derived from 5,6-dihydroxyindole (DHI; for simplicity named also hydroquinone, HQ) and 5,6-dihydroxyindole-2-carboxylic acid (DHICA) [4]. The detailed structural properties of this polymer are still under study because of unclear covalent and ionic configurations of HQ and DHICA monomers within the natural eumelanin unit. It is possible, however, to produce synthetically pure DHI or DHICA melanin. In this respect, theoretical studies presented in this paper relate to synthetic eumelanins that are free or almost free from the DHICA contribution in the structure.

Absorption bands of eumelanins have been recently [5–7] shown to depend on different levels of aggregation reported in scanning electron microscopy studies. The proposed aggregation structure is generally viewed as a molecular system containing 3–4 oligomers, often referred to in literature [6,7] as the fundamental aggregate. The hypothetical pigment structure is then believed to be assembled from these π stacked, cross-linked units. In an earlier attempt to explain electronic (and optical) properties of melanins (*cf.* Fig. 2), a band model [8,9] viewing melanins as amorphous semiconductors has been proposed. In fact, melanins can be considered as mixtures of more or less similar polymers, apparently made up of different structural units linked through heterogenous non-hydrozable bonds. The latter are the result of the polymerization of indole-type rings in both, the quinone and hydroquinone oxidation state, randomly cross-linked and piled. Theoretical contributions on a speculative model [10, 11] pictured eumelanins as a linear chain semiconducting polymer. Extrapolating the bonding character of the lowest unoccupied molecular orbital (LUMO) of one particular dimer of 5,6-indolequinone to the lowest conduction band of the infinite polymer,

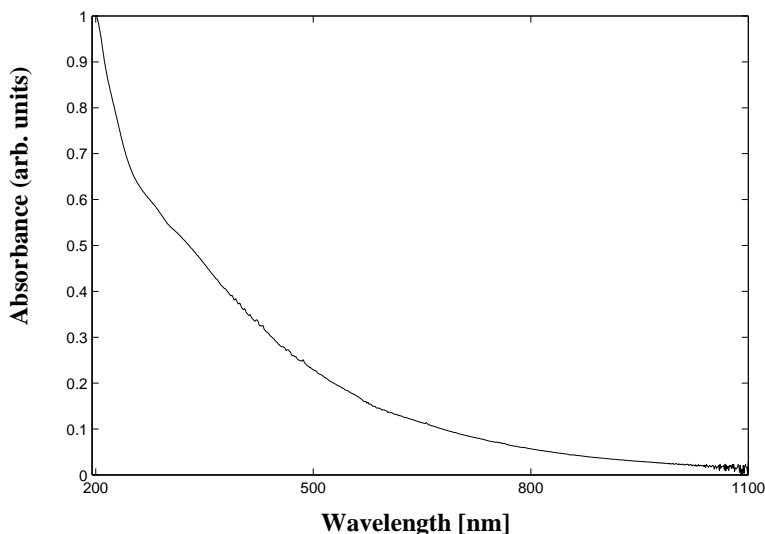


Fig. 1. Experimental steady state absorption spectrum of synthetic DOPA melanin recorded using a UV-Vis spectrophotometer with an accuracy of 2nm.

Pullman and Pullman [11] have pointed out the tendency of such a melanin model to be an electron acceptor that could explain trapping of free radicals characteristic for the natural and synthetic pigments.

More recent studies along similar lines have been performed by Galvão and Caldas [12–14]. Using the Hückel π -electron approximation and the parametrization of Pullman [11], the authors studied the electronic structure of a family of ideal ordered polymers arising from the indolequinone in different redox states. It has been shown that the direction of polymerization begins to emerge as the length of the polymer increases. The authors pointed out also that the redox state of the melanin units played a role in its band structure, as *e.g.* the polymer built from 5,6-dihydroxyindole units exhibited larger gaps and narrower bands, whereas finite chains of semi-quinone units exhibited bonding character of their LUMO.

Some limitation of this approach is the assumption of planarity of melanin polymers, which in most cases does not need to be the case. In fact, structural modeling of eumelanins based on comparing calculated data of the reduced structure factor and radial distribution function for limited random network models with the experimental X-ray scattering data [15] suggest that planar models consisting of undistorted long chains are not appropriate structures for amorphous melanins. We have thus considered the role of conformational variations of eumelanins' oligomers in modifying and modulation of their light-absorption properties. According to the existing

evidence [1–3, 16, 17] that the 5,6-indolequinone (IQ) or the reduced forms, semi-quinone (SQ) and hydroquinone (HQ) compose the major part of the active pigment, these three basic units (*cf.* Fig. 1) in their neutral forms have been used to build up model polymeric structures.

When focusing on oligomeric models of eumelanins, we have assumed in consistency with the wide-angle X-ray diffraction measurements of synthetic eumelanin samples and scanning electron microscopy images of monolayers of synthetic eumelanins on graphite [5, 15], that a fundamental building block of the polymer is a structure consisting of several (4–10) 5,6-indolequinone residues composed in π -system molecular stacks. Therefore, as a starting model unit for a higher order polymeric structure of eumelanin a pentamer containing HQ, IQ or SQ molecules has been chosen and subsequently used to analyze randomly created structures of various conformations. Pentamer structures with various proportions of HQ, IQ and SQ content have been constructed from geometrically optimized monomers and further analyzed for their spectroscopic properties. All oligomer models have been built by using “Random Polymer Builder” module of the Cerius²/MSI packet [23].

In assessing electronic spectral properties of modeled molecular structures, we report here results from the spectroscopic ZINDO/s calculations developed by Zerner [18] and co-workers. The method is based on re-parametrization of the semi-empirical INDO (Intermediate Neglect of Differential Overlap) approach that includes monoatomic differential overlap for one-centre integrals (*i.e.* integrals involving basis functions on the same atom). These calculations yield absorption maxima which establish that the differences in mixing ratios of various monomeric units in an overall polymeric structure of eumelanins can influence and alter absorption spectrum of the oligomer.

2. Computational models

In order to pinpoint the factors controlling the spectra of eumelanin polymers, the model subunits have been treated at several levels of structural elaborations. As basic components of eumelanins 5, 6-dihydroxyindole (HQ), 5,6-indolequinone (IQ) and semiquinone (SQ) (see Fig. 2.) have been chosen. Since experimental data on the geometry of the molecules in Fig. 2 are not available, the bare skeletons of indole molecules have been edited by a molecular editor in the InsightII/MSI module and further geometrically optimized by use of either *ab initio* Gaussian-94 [19] or semiempirical consistent valence forcefield (CVFF) method. In both cases the energies for conformation were minimized until the convergence was achieved (the maximum derivative was less than $0.0001 \text{ kcal mol}^{-1} \text{ \AA}^{-1}$). The augmented CVFF program has been developed for material science applications [20]

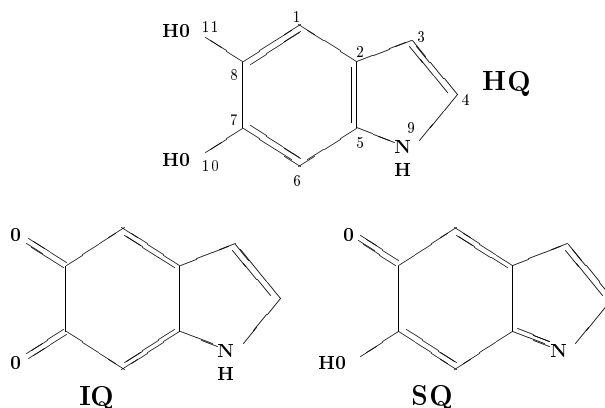


Fig. 2. Schematic monomer structures used in this work and labeling of active sites: HQ- hydroquinone; IQ-5, 6-indolequinone; SQ-semiquinone.

and is considered a standard forcefield to be used for organic molecules and polymers. As a default forcefield in Discover 95.0 molecular dynamics simulation package, it has been extensively used over the past years and is usually considered [20, 22, 23] well tested and characterized. It is primarily intended for studies of structures and binding energies, although is known also to predict satisfactorily frequencies in vibrational spectra as well as conformational energies. Structures optimized by CVFF method have been further used as input parameters for spectroscopic ZINDO [18] calculations. The method circumvents cumbersome and time-consuming *ab initio* treatment of complex systems and is one of commonly used semiempirical molecular orbital (MO) methods. Over the last decade it has been successfully applied in the study of bulk solids and defects in semiconductors [21]. The INDO electronic calculations are based on an all-valence-electron, self consistent field (SCF) molecular orbital procedure with the configuration interaction (CI). Within the general MO method, the Fock matrix can be represented as

$$F_{\mu\nu} = h_{\mu\nu} + \sum_{\lambda,\sigma}^N P_{\lambda,\sigma} [(\mu\nu|\lambda\sigma) - \frac{1}{2}(\mu\lambda|\nu\sigma)] , \quad (2.1)$$

where $h_{\mu\nu}$ stands for the core integral

$$h_{\mu\nu} = \int \phi_{\mu}(1) H_{\text{core}} \phi_{\nu}(1) d\tau_1 , \quad (2.2)$$

$(\mu\nu|\lambda\sigma)$, $(\mu\lambda|\nu\sigma)$ represent two-electron Coulomb integral and the exchange integral, respectively,

$$(\mu\nu|\lambda\sigma) = \int \int \phi_\mu(1)\phi_\nu(1)r_{12}^{-1}\phi_\lambda(2)\phi_\sigma(2)d\tau_1d\tau_2. \quad (2.3)$$

The electron density matrix $P_{\lambda\sigma}$

$$P_{\lambda\sigma} = 2 \sum_{i=1}^{\text{occ}} c_{\lambda i}^* c_{\sigma i}, \quad (2.4)$$

contains molecular orbital expansion coefficients $c_{\lambda i}$ of the Ψ_i orbital formed as a linear combination of basis functions ϕ_λ . The variation principle $\partial E/\partial c_{\mu i} = 0$ applied to a closed-shell system leads then to the Roothaan–Hall equations

$$\sum_{\nu=1}^N (F_{\mu\nu} - \varepsilon_i S_{\mu\nu}) c_{i\nu} = 0, \quad (2.5)$$

for the set of orbital energies ε_i and MO coefficients $c_{i\nu}$. The elements of the matrix $S_{\mu\nu}$ are the atomic orbital (AO) overlap integrals $\int \phi_\mu^*(1)\phi_\nu(1)d\tau$.

Eq. (2.5) is solved iteratively until a self-consistency is reached within the demanded accuracy. The final SCF solution yields desired MOs Φ_i and their orbital energies ε_i . The ground state electron configuration is produced by filling the orbitals with all electrons in the order of increasing energy.

The SCF calculations done with a set of M basis functions require the computation of M^4 matrix elements. In order to make a treatment of large molecules possible, one has to reduce the complexity by either replacing the effect of inner core electrons by effective (pseudo-) potentials or by applying the semi-empirical SCF method which neglects most of the matrix elements $(\mu\nu|\lambda\sigma)$ and parametrize the remaining ones. The term “intermediate neglect” points to the retention of one-center-two-electron exchange integrals $(\mu\nu|\mu\nu)$. Within the Zerner’s version of INDO (ZINDO) approximation [18], basis orbitals ϕ_i are envisioned to be strongly orthogonal and they obey the relations

$$\begin{aligned} (\mu^A\nu^B|\lambda^C\sigma^D) &\equiv \delta_{AB}\delta_{CD} \int \int \phi_\mu^A(1)\phi_\nu^B(1)r_{12}^{-1}\phi_\lambda^C(2)\phi_\sigma^D(2)d\tau_1d\tau_2 \\ &= (\mu^A\nu^A|\lambda^A\sigma^A) \quad A = C, \\ &= (\mu^A\nu^A|\lambda^C\sigma^C) \quad A \neq C, \end{aligned} \quad (2.6)$$

where ϕ_μ^A is the atomic orbital centered on atom A . In order to maintain rotational invariance, two-center integrals ($A \neq C$) are evaluated over atomic orbitals $\tilde{\phi}_\mu^A$ that are s symmetric but have the same exponents and expansion

coefficients as ϕ_{μ}^A . The one-center core integrals $h_{\mu\mu}$ are obtained from ionization potentials and the resonance integrals (the two-center $h_{\mu\nu}$ integrals) are purely empirical parameters set to reproduce experimental spectra. The method as employed herein leads to the ground electronic states obtained as closed-shell molecular orbital wave functions in the restricted Hartree–Fock (HF) framework. In the next step, low lying excited states were approximated by configuration interactions (CI) among configurations generated as single excitations from restricted HF ground state. The CI method included the highest 15 occupied and lowest 15 unoccupied molecular orbitals¹.

All polymers were arbitrarily chosen as pentamers built by use of the “Random Polymer Builder” module of the MSI packet [23]. Four different groups of polymers: homogenous polyHQ, polySQ, polyIQ (*cf.* Fig. 3) and heteropolymers (*i.e.* pentamers built up from basic units with random ratios of molecules HQ:IQ:SQ) were investigated. The polymer structures were formed by defining all possible pairs of “head” and “tail” positions out of 5 labeled centers (see Fig. 2) located on a monomer. Structural configuration models of pentamers have been then developed along the poly-

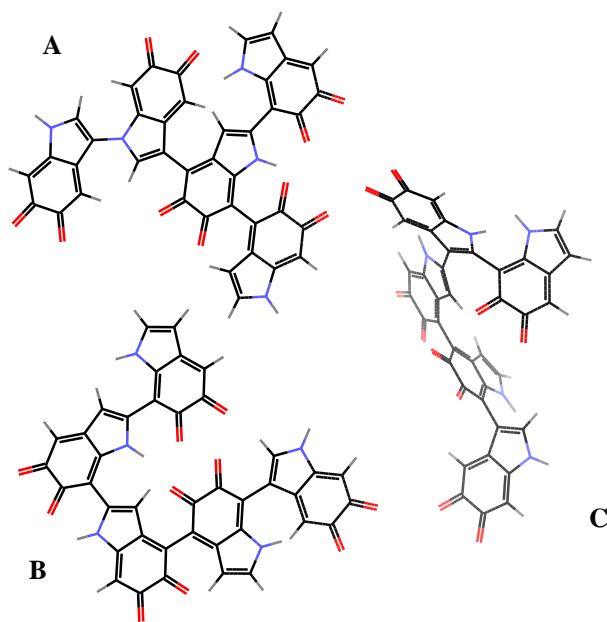


Fig. 3. Examples of polymers used in calculations: A — planar and forked, B — planar and linear, C — nonplanar, linear.

¹ Expanding the active basis of the CI space have not resulted in significant differences in modeled absorption spectra, therefore, all oligomeric structures have been treated within the same CI-conformity.

merization direction in which “heads” were joined with “tails” of subsequent monomers. Resulting pentamer structures (*cf.* Fig. 3) can be either linear and flat, nonplanar linear or forked structures, respectively. Despite their various conformational structures, all three groups are characterized by a mean dimension (measured as a maximum observable distance between non-hydrogen atoms in a model pentamer form) of about 2 nm and molecular weight about 720–740, *i.e.* with $MW < 1000$. If assuming that such units are basic chromophores in the eumelanin structure, the models predict that there are about of million of such pentamers in a melanin subunit of an average diameter 150–200 nm [15,24].

Heteropolymeric structures have been created either with equal probabilities of choosing IQ, SQ or HQ molecule at each step of polymerization, or by using IQ and HQ monomers only, *i.e.* with the HQ:IQ:SQ probability proportion taken as 3:1:0. The latter choice switches off the reduced form of IQ, the component SQ, that is mainly responsible for formation of free radicals produced during melanin synthesis [2]. The planar and non-planar conformations were analyzed seeking for their effect on absorption spectra. Models of planar linear polymers (each monomer had no more than 2 bonds), planar forked polymers and non-planar linear polymers (see Fig. 3) have been investigated for their absorption spectra, calculated solely for neutral structures by using ZINDO-CI method.

Dynamic interactions between the model basic “molecule” and the surrounding medium (composed of the set of randomly distributed similar oligomeric units) can be a source of fluctuations in the electronic gap energy between the ground and excited state. To account for these fluctuations and their effect on the system response to a radiation field, we have presented calculated spectra adopting a Brownian oscillator model [25] that relates variability in the electronic gap to displacements in some dynamical variable x representing the system under consideration. In the linear regime (weak coupling to the perturbing external radiation field), the fluctuation-dissipation theorem relates the system’s response function to the derivative of the correlation function $C(t' - t) = \langle x(t)x(t') \rangle$ with brackets representing an equilibrium average. In the Brownian oscillator model the equilibrium states are defined by incorporating a model of the bath represented by a Gaussian stochastic force $f(t)$ acting on a variable x

$$m_i \ddot{x}_i(t) + m_i \omega_i^2 x_i(t) + m_i \int_{-\infty}^t d\tau \gamma_i(t - \tau) \dot{x}_i(\tau) = f_i(t) + F_i(t), \quad (2.7)$$

where m_i , $F_i(t)$ stand for the “mass” of a mode x_i and an external driving force, respectively. The correlation of the random force is related to the

dissipative term (friction), *i.e.* $\langle f_i(t)f_k(t') \rangle = \delta_{ik}2m_i k_B T \gamma_i(t-t')$. The variation of the friction term with time (or frequency) reflects the timescale of the thermal motions of the bath. By assuming that the latter are very fast compared to the oscillator motion, we accept the ohmic dissipation model with γ_i being a constant. In a strongly over-damped case ($\gamma_i \gg 2\omega_i$) and in a fast modulation limit [25], the absorption lineshape calculated as

$$\sigma_{\text{abs}}(\omega) = \frac{1}{\pi} \text{Re} \int_0^{\infty} dt \exp[i(\omega - \omega_{eg})t] \exp[-g(t)], \quad (2.8)$$

with

$$g(t) \equiv \int_0^t dt_2 \int_0^{t_2} dt_1 C(t_1), \quad (2.9)$$

assumes a Lorentzian form

$$\sigma_{\text{abs}}(\omega) = \frac{\Gamma}{\pi[(\omega - \omega_{eg})^2 + \Gamma^2]}, \quad (2.10)$$

with the line width Γ proportional to the product of characteristic nuclear time scale (characteristic time scale of medium relaxation) and a coupling strength of the nuclear degrees of freedom to the electronic transition. Without discussing the origin of the particular choice of the lineshape in more details, we have thus arbitrarily adopted that the energy transitions calculated for the model system were Lorentzian enveloped and summed, weighted with an oscillator strength to simulate the overall absorption spectra. Differently chosen values of Γ reflect then the degree of dissipation of absorbed energy via coupling to the bath.

3. Results

3.1. Monomers

Geometrical features of the ground state monomers used in this study have been compared with optimized coordinates from *ab initio* Gaussian 94 calculations. In accordance with the previous analysis by Bolivar-Marinez *et al.* [14], various methods of optimization result in small variation of main bond lengths and bond and dihedral angles yielding structures that are basically planar. This feature is further reflected in the major $\pi - \pi^*$ character of the transition between highest occupied (HOMO) and lowest unoccupied (LUMO) molecular orbitals for all monomer molecules. To assess the reliability of our calculations based on CVFF method combined with ZINDO/s calculations in predicting spectral features of melanin's derivatives, we have

calculated transition energies for the bare skeleton of HQ (with each omitted substituent replaced by a hydrogen atom), after optimization by either CVFF or PM3 method which has been used in a previous study [14]. The first transition line calculated in ZINDO was 306.5 nm (296.6 nm) for the structure optimized with CVFF (PM3) program, respectively. This has been compared with the first transition line (300.3 nm) calculated for the “empirical” bare skeleton structure of tryptophan obtained from the Protein Data Bank.

In all these cases, the first transition lines were predicted with oscillator strengths of about 0.02. By inspection, all structures displayed also similar character of the calculated CI coefficients and were comparable with the previous theoretical [14] and experimental [17] works related to melanin’s monomers.

Results of Gaussian/ZINDO and CVFF/ZINDO calculations on neutral HQ, IQ and SQ monomers are presented in Table I. The first optically active electronic transitions (first row entry in Table I) and the strongest active electronic transition (second row entry in Table I) exhibit shifts towards longer wavelengths after CVFF structure optimization which allows structures with some degree of non-planarity².

TABLE I

Calculated excitation energies [nm] for optimized structures of melanin’s precursors. First row: first transition, second row: strongest transition. Oscillator strength are given in paranthesis.

monomer	Gaussian/ZINDO	CVFF/ZINDO
	energy (osc. strength) [nm]	energy (osc. strength) [nm]
HQ	307.2(0.05)	316.2(0.06)
	228.0(0.82)	232.6(0.87)
IQ	464.5(0.12)	529.9(0.13)
	218.9(1.03)	225.3(0.52)
SQ	481.0(0.02)	856.4(0.03)
	217.4(0.94)	238.2(1.46)

² As it has been documented elsewhere [27], conformational distortions from planarity in conjugated systems of atoms may influence the π -pattern of frontier orbitals and result in red-shifted excitation energies. The effect seems to be the strongest for the semiquinone (SQ) molecule with geometry optimized by the CVFF force field.

Reported transitions are dominated by a few configurations involving frontier orbitals. Inspection of the calculated CI coefficients reveals that about 70% of the first excited state for HQ monomer is accounted for by HOMO→LUMO excitation and about 15% of HOMO−1 →LUMO+1 excitation. The strongest transition is composed of mixing among 2 highest occupied and 3 lowest unoccupied orbitals. The pattern of the first excited state is essentially preserved for SQ and IQ monomers where >96% of excitation comes from HOMO→LUMO transition with remaining excitations contributing with less than 1%.

3.2. Oligomers and polymers

Fig. 4 presents simulated optical absorption spectra of model polymers. The curves have been obtained from the optical transition spectrum enveloped by normalized Lorentzians weighted by the calculated oscillator strength; *i.e.* energies (λ_i) and oscillator strengths (s_i) obtained from calculations were converted to

$$\sigma_{\text{abs}}(\lambda) = \sum_i \frac{s_i}{(\lambda - \lambda_i)^2 + 10^2} \quad (3.1)$$

with the width of a line set up arbitrarily to 10 (in units of λ). The graphs refer to spectra of different mixtures of polymers: the first column displays spectra of the uniform mixture of polyHQ polymers (*i.e.* pentamers composed of HQ monomers, only), second and third columns show absorbance spectra of similar uniform mixtures of polyIQ and polySQ, respectively. The fourth column presents spectra of heteropolymers composed with equal probabilities of choosing either one of three various monomers (*i.e.* with HQ:IQ:SQ = 1:1:1) at each step of the “polymerization process” leading to a basic pentamer structure. The last column displays spectra of nonuniform polymers built by use of the proportion HQ:IQ:SQ = 3:1:0 at the basic level of modelling. Rows in Fig. 4 relate to spectra obtained for different conformations of polymers. The first row represents mixtures of linear and planar polymers (*cf.* Fig. 3), the second and third row display spectra of linear nonplanar and planar forked polymers, respectively.

All spectra up to the last row in Fig. 4 have been calculated as mixtures of 15 pentamers, whereas the bottom row shows sums of simulated spectra for 45 polymers whose absorbance spectra are displayed in upper three rows of each column. As an example, the third column and second row of Fig. 4 displays spectrum of 15 linear, nonplanar pentamers composed of SQ monomers, only. Accordingly, the inlet in 5th column and 3rd row presents absorption spectrum of 15 “forking” pentamers composed of HQ and IQ molecules taken in proportion 3:1 (with no contribution of SQ molecules). Sum of spectra for various conformational structures of that type is displayed in the bottom right corner of Fig. 4.

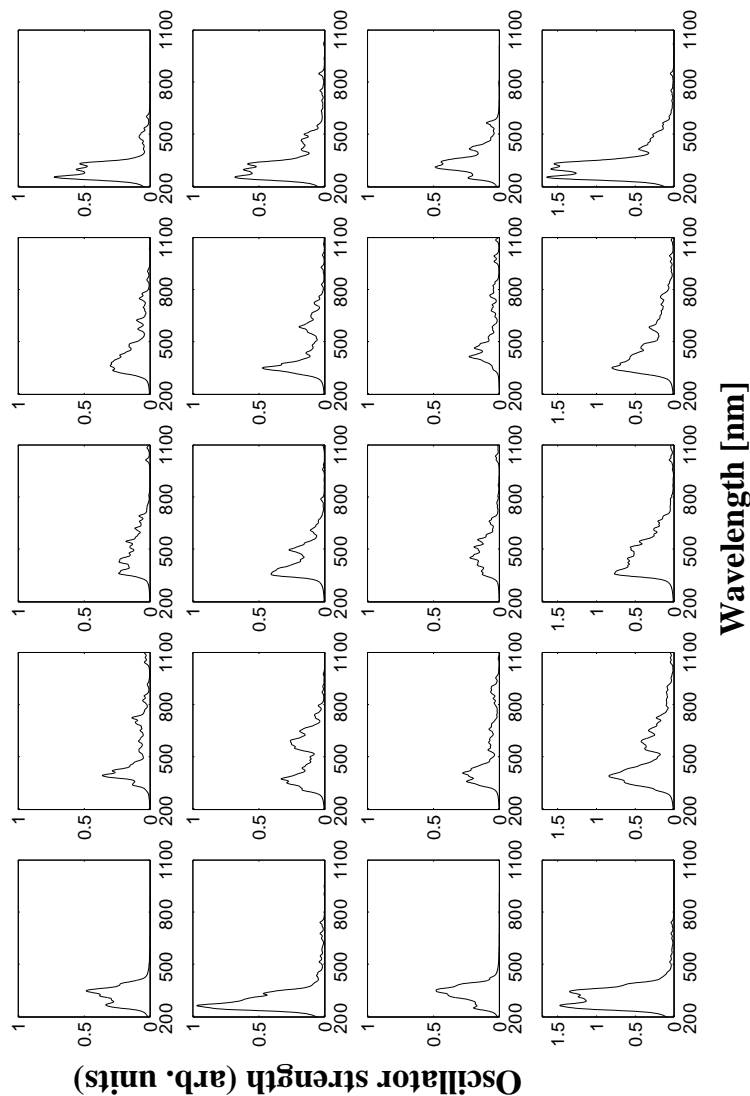


Fig. 4 Theoretical absorption spectra for different mixtures of polymers: first column — polyHQ, second column — polyIQ, third column — polySQ, fourth and fifth columns — heteropolymers (HQ:IQ:SQ = 1:1:1 and HQ:IQ:SQ = 3:1:0, respectively). Rows refer to different conformational forms: first row — spectra of 15 linear planar polymers, second row 15 — linear non planar polymers, third row — 15 forked planar polymers. Last row represents sums of spectra in each column (45 polymers).

As can be inferred from Fig. 4, spectra of polyHQ have dominant contributions within the range 200–400 nm, whereas admixture of IQ or SQ components results in a red shift of the absorption lines. Conformation variations seem to result in varying intensity of absorption, it is ambiguous however, to conclude on the overall effect of conformations on spectra of model polymers.

Fig. 5 comprises model absorption spectra of “higher order” polymers: in the top left corner spectra of 45 polyHQ and 45 polyIQ oligomers are displayed, second position in the first column represents spectra of 45 polyHQ and 45 polySQ, whereas the bottom of first column contains simulated spectra for mixture of 45 polyIQ and 45 polySQ polymers. For comparison, spectra of mixture of three uniform oligomers (45 polyHQ + 45 polyIQ + 45 polySQ) have been displayed (second column and first row in Fig. 5) along with 45 heteropolymers HQ:IQ:SQ = 1:1:1 (second row) and 45 nonuniform oligomers HQ:IQ:SQ = 3:1:0 (second column, third row). Note that all “higher order” spectra of polymers are constructed as direct sums (mixtures) of spectra of pentamers and as such they do not take into account interactions among those units.

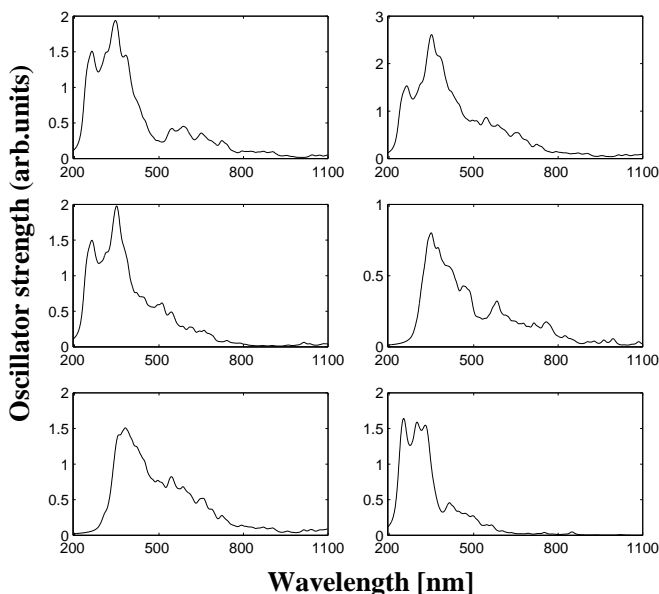


Fig. 5. Simulated spectra for ‘higher order’ mixtures of polymers: left column, top — 45 polyHQ + 45 polyIQ, below — 45 polyHQ + 45 polySQ, bottom — 45 polyIQ + 45 polySQ. Right column — 45 polyHQ + 45 polyIQ + 45 polySQ, below — 45 heteropolymers (HQ:IQ:SQ = 1:1:1), bottom — 45 heteropolymers (HQ:IQ:SQ = 3:1:0). See text for details.

Simulated optical absorption spectra suggest that the main contribution to the absorption in the range of 500–800 nm may be attributed to the presence of SQ molecules in oligomeric structures. Shape of simulated spectrum of mixtures of nonuniform polymers resembles experimental spectrum (Fig. 1) for synthetic DOPA melanin. The maximum intensity of modelled spectrum is, however, shifted to about 300 nm, whereas the peak intensity in the experimental spectrum is observed already at 200 nm. It can be expected that additional modulation of spectrum may arise from some environmental effects. For example, presence of localized charges may be a source of electrochromic shift in the spectrum with red or blue shifts in transition energies determined by the sign and location of charges [26,27]. Possible shifts in transition energies of model polymers may be also induced by higher content of charged forms of IQ monomers in model structures. In particular, it has been demonstrated in the previous theoretical study by Bolivar-Marinez *et al.*, [14] that negative ions of IQ, SQ and HQ molecules (-1) begin to absorb at about 1.0 eV. This effect is responsible, however, for the red shift in simulated optical absorption spectra of negatively charged monomers.

Calculated optical spectra smoothen also and shift when assuming stronger dissipation of excitation energies in the system, resulting in a broader width of lines (see Fig. 6). In the case of heterogeneous oligomers models (HQ : IQ : SQ = 3 : 1 : 0) fourfold higher line width parameter than originally

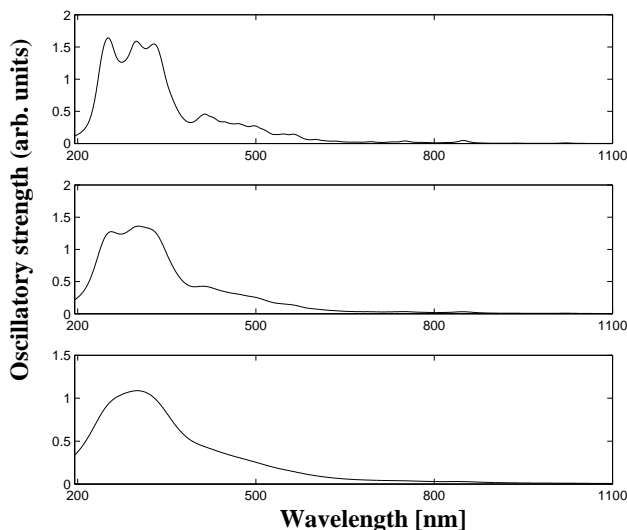


Fig. 6. Effect of assumed line width on spectra of 45 heteropolymers (built from HQ and IQ monomers only). Starting from the top, the values of Lorentzian's widths have been set up to 10, 20 and 40 (in units of the wavelength), respectively.

chosen leads to a single humped spectrum with a broad, structureless tail. The effect, however, does not alter significantly absorbance in the 200 nm region.

Synthetic *eumelanin* whose properties have been modelled in this study lacks a protein coat and, therefore, its optical spectrum does not match the natural pigment, especially in the region about 250–270 nm, where existing evidence [24] of spectral features has been attributed to absorption of light by protein environment.

4. Conclusions

The absorption spectra for model of *eumelanins* were calculated assuming melanin to be composed of mixture of various unit-polymers. All molecules were parametrized as random pentamers of HQ, SQ and/or IQ. The idea of “mixed nature” of the pigment, composed of heterogeneous oligomers in a random, not necessarily well organized assemblies is compatible with experimental data. Simulated optical spectra manifest the effect of aggregation in oligomer conformation resulting in broadening of the absorbance arm in the region of 500–800 nm. Peak intensity of spectra can be correlated with the presence of neutral HQ monomers in model structures. At higher level of aggregation (135 pentamers and more), further addition of a polymeric unit (a pentamer) to the existing structure does not alter the character of the spectrum. Also, conformational deformations of constituents (oligomers) have only a minor effect on the structure of modelled optical spectra. Our future studies aim at understanding stabilisation of radicals in a system of stacked oligomers and interpretation of factors responsible for radical-trapping processes in eumelanins.

The authors acknowledge many fruitful discussions with Prof. Tadeusz Sarna and Dr Albert Wielgus who has kindly provided the experimental spectrum for the synthetic DOPA melanin. K.B. acknowledges hospitality of Prof. J. Brickmann and the group of Physical Chemistry II at the TU Darmstadt where part of computational analysis has been performed. This work has been supported by the Marian Smoluchowski Institute of Physics Research Grant (1999–2002).

REFERENCES

- [1] G. Prota, *Melanins and Melanogenesis*, Academic Press, New York 1992.
- [2] T. Sarna, H.M. Swartz, *The Physical Properties of Melanins*, in *The Pigmentary System — Physiology and Pathology*, Ed. J. Nordlund, R. Boissy, V. Hearing, R. King and J-P. Ortonne, Oxford University Press, Oxford 1998, p. 333.

- [3] G. Prota, M. D'Ischa, A. Napolitano, *The Chemistry of Melanins and Related Metabolites*, in *The Pigmentary System — Physiology and Pathology*, Ed. J. Nordlund, R. Boissy, V. Hearing, R. King and J-P. Ortonne, Oxford University Press, Oxford 1998, p. 307.
- [4] S. Ito, *Biochim. Biophys. Acta* **883**, 155 (1986).
- [5] Z.W. Zajac, J.M. Gallas, J. Cheng, M. Eisner, S.C. Moss and A.E. Alvarado-Swaisgood, *Biochim. Biophys. Acta* **1199**, 271 (1994).
- [6] C.M. Clancy, J.B. Nofsinger, R.K. Hanks, J.D. Simon, *J. Phys. Chem.* **B104**, 7871 (2000).
- [7] J.B. Nofsinger, J.D. Simon, *Photochem. Photobiol.* **74**, 31 (2001).
- [8] J.E. McGinnes, *Science* **177**, 896 (1973).
- [9] P. Proctor, J.E. McGinnes, P. Corry, *Science* **183**, 853 (1974).
- [10] H.C. Longuet-Higgins, *Arch. Biochem. Biophys.* **54**, 384 (1960).
- [11] B. Pullman, A. Pullman, *Quantum Biochemistry*, Academic Press, New York 1965; A. Pullman, B. Pullman, *Biochim. Biophys. Acta* **54**, 384 (1961).
- [12] D.S. Galvão, M.J. Caldas, *J. Chem. Phys.* **92**, 2630 (1990).
- [13] D.S. Galvão, M.J. Caldas, *J. Chem. Phys.* **93**, 2848 (1990).
- [14] L.E. Bolivar-Marinez, D.S. Galvão, M.J. Caldas, *J. Phys. Chem.* **103**, 2993 (1999).
- [15] J. Cheng, S.C. Moss, M. Eisner, *Pigment Cell Res.* **7**, 263 (1994).
- [16] A. Young, *Phys. Med. Biol.* **42**, 789 (1997).
- [17] X. Zhang, C. Erb, J. Flammer, W. Nau, *Photochem. Photobiol.* **71**, 524 (2000).
- [18] J. Ridley, M. Zerner, *Theor. Chem. Acta* **72**, 867 (1987).
- [19] www.gaussian.com; M.J. Frisch, E. Frisch, J.B. Foresman, *Gaussian 94 User's Reference*, Manual Version, Gaussian Inc. 1996.
- [20] P. Dauber-Osguthorpe, V. Roberts, D. Osguthorpe, J. Wolff, M. Genest, A. Hagler, *Proteins: Str. Funct. Genetics* **4**, 31 (1988).
- [21] A. Stashans, M. Kitamura, *Solid State Commun.* **99**, 583 (1996); P. Fulde, *Electron Correlations in Molecules and Solids*, Springer Verlag, Heidelberg 1995.
- [22] J. Maple, U. Dinur, A. Hagler, *Proc. Nat. Acad. Sci.* **85**, 5350 (1988).
- [23] Molecular Simulations Inc., *System Guide for InsightII Products*, Release 4.0, San Diego: Molecular Simulations Inc., 1999.
- [24] J.D. Simon, *Acc. Chem. Res.* **33**, 307 (2000).
- [25] S. Mukamel, *Principles of Nonlinear Optical Spectroscopy*, Oxford University Press, New York 1995.
- [26] L.K. Hanson, J. Fajer, M.A. Thompson, M.C. Zerner, *J. Am. Chem. Soc.* **109**, 4728 (1987).
- [27] E. Gudowska-Nowak, M.D. Newton, J. Fajer, *J. Phys. Chem.* **94**, 5795 (1990).